DOI: 10.5604/01.3001.0015.5065

Volume 108 • Issue 2 • October 2021

Journal of Achievements in Materials and Manufacturing Engineering

International Scientific Journal published monthly by the World Academy of Materials and Manufacturing Engineering

Static response of curved steel thin-walled box-girder bridge subjected to Indian railway loading

V. Verma [a,*], K. Nallasivam [b]

[a] Research Scholar, Department of Civil Engineering , National Institute of Technology, Hamirpur-177005, India

[b] Assistant Professor, Department of Civil Engineering, National Institute of Technology, Hamirpur-177005, India

* Corresponding e-mail address: virajan75409@gmail.com

ORCID identifier: https://orcid.org/0000-0002-4673-8209 (V.V.)

ABSTRACT

Purpose: The primary objective of the current study is to numerically model the steel thin-walled curved box-girder bridge and to examine its various response parameters subjected to Indian Railway loading.

Design/methodology/approach: The analysis is conducted by adopting a one dimensional curved thin-walled box-beam finite beam element based on finite element methodology. The scope of the work includes a computationally efficient, three-noded, one-dimensional representation of a thin-walled box-girder bridge, which is especially desirable for its preliminary analysis and design phase, as well as a study of the static characteristics of a steel curved bridge, which is critical for interpreting its dynamic response.

Findings: The analytical results computed using finite element based MATLAB coding are presented in the form of various stress resultants under the effect of various combinations of Indian Railway loads. Additionally, the variation in different response parameters due to changes in radius and span length has also been investigated.

Research limitations/implications: The research is restricted to the initial design and analysis phase of box-girder bridge, where the wall thickness is small as compared to the cross-section dimensions. The current approach can be extended to future research using a different method, such as Extended finite element technique on curved bridges by varying boundary conditions and number of elements.

Originality/value: The validation of the adopted finite element approach is done by solving a numerical problem, which is in excellent agreement with the previous research findings. Also, previous studies had aimed at thin-walled box girders that had been exposed to point loading, uniformly distributed loading, or highway truck loading, but no research had been done on railway loading. Moreover, no previous research had performed the static analysis on thin-walled box-girders with six different response parameters, as the current study has. Engineers will benefit greatly from the research as it will help them predict the static behaviour of the curved thin-walled girder bridge, as well as assess their free vibration and dynamic response analysis.

Keywords: Steel box-girder bridge, Thin-walled structures, Finite element technique, MATLAB, Torsional bi-moment

Reference to this paper should be given in the following way:
V. Verma, K. Nallasivam, Static response of curved steel thin-walled box-girder bridge subjected to Indian railway loading, Journal of Achievements in Materials and Manufacturing Engineering 108/2 (2021) 63-74. DOI: https://doi.org/10.5604/01.3001.0015.5065

ANALYSIS AND MODELLING

1. Introduction

The thin-walled beam sections have become extremely prevalent in the construction of modern engineering structures owing to their lighter weight and longer spans. Over the last few years, the concept of horizontally curved thin-walled box-girder bridges has taken giant strides thanks to their high flexural and torsional resilience. Curved box girders are vulnerable to complicated structural actions of torsion and distortion warping, in addition to the usual extension and bending effects. The area of curved box-girder bridges may indeed seem intriguing, but it poses enormous challenges for engineers for their research and design. Extensive research has been published in the literature on the analysis of thin walled box-girder bridges. Vlasov [1] extensively explained the theory for thin-walled beams, which divided torsional moment into pure and warping components. Maisel [2] modified the general coordinate approach of Vlasov to compensate torsional and distortional effects in thin-walled box beams. The impact of shear lag on thin-walled box-girder bridges was thoroughly investigated by [3,4]. Jonsson [5] provided a systematic method for distortion of thin-walled beam, in which a general differential equation was formed to determine warping displacement. Ezeokpube *et* al. [6] presented experimental and computational simulations for the static response of thin-walled box girder bridges. Kashefi *et* al. [7] had experimentally examined the static and vibrational characteristics of straight and curved thin-walled box beams. Numerous theories and analytical methods have been formulated for the analysis of box-girder bridges, but the approach to finite element analysis is generally considered to be the most robust. Fam and Turkstra [8] introduced a box-bridge finite element scheme model featuring arbitrary combinations of straight and horizontal curved sections. Boswell and Zhang [9] used finite element methodology to address the distortion problem in thin-walled box spine beams. Kim and Kim [10] introduced C_o–continuous displacement based box beam finite element for static and dynamic analysis of traditional box bridges. Begum Z [11] made use of the commercially available FEM software ANSYS to examine the behaviour of steel box girder bridges. Zhu *et* al. [12] successfully used the finite element method for the vibrational analysis of thin walled rectangular beams. Gupta and Kumar [13] estimated the flexural response of curved box- girder bridges using commercially available FEM software CSiBridge. Hamza *et* al. [14] used a non-linear finite element approach to evaluate the ultimate load capacity for horizontally curved box steel beam.

1.1. Need of present study

Various researchers had developed a large number of finite elements for the analysis of box-girder bridges. A technique was needed, as many of them did not fully reflect all the complex structural actions of a curved box-girder bridge, however the three noded 1D beam element developed by [15], which was also used by [16], was found to represent all of the complex structural actions. Also, shell elements were considered the best for an accurate analysis of curved box-girder bridge, but the overall degrees of freedom with these elements were much higher, resulting in higher computational costs. During the preliminary design phase, such a detailed analysis was not required and a simple, cost-effective 1D approach was needed, which has been applied in the present study.

Research gap

Most of the researchers listed above had studied the thin-walled box-girders which were either subjected to point loading, uniformly distributed loading, or highway truck loading; however, no analysis was conducted with regard to railway loading. Also, none of the previous researchers had statically analysed thin-walled box-girders with six different response parameters, which has been done in the work presented.

1.2. Objectives

1. Modeling one-dimensional finite element thin-walled box beam elements for curved steel box-girder bridge in a computationally efficient manner.
2. Static response analysis of a curved steel thin-walled box-girder bridge exposed to Indian Railway loads.
3. Investigating the changes in response parameters caused due to variations in radius and span length of a curved steel box-girder bridge subjected to Indian railway loading.

2. Methodology of a thin-walled box-girder using finite elements

2.1. Geometry of the element

Figure 1 shows a thin-walled box beam element with some curvature where the cross-sections are created using straight lines. The cross-sectional symmetry axis is presumed to be vertical in order to make the study of distortions simple. This assumption becomes redundant while performing torsion and bending analysis.

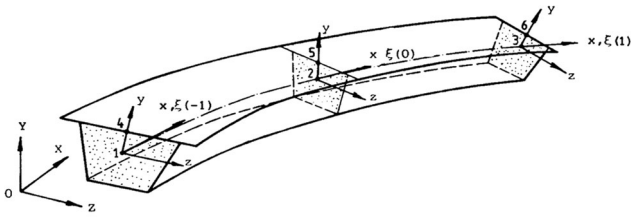

Fig. 1. Three noded thin-walled box beam element

The element axis is defined as the locus of the centroids which may be eccentric from but parallel to the flexural axis. Three elemental nodes are located on the axis, two at the ends and one at the mid-point.

The element is formulated by a local Cartesian coordinate system (x, y, z) which is in the direction of axis curve. The centroid of the cross-section denotes the origin of the coordinate system and it is assumed that the principal axes of the cross-section coincides with the direction of local yz axes. The local x axis is tangent to the axis of the element. The direction of the tangent is from the first node towards the third one. The vertical axis of symmetry is represented by the local y axis and a right handed orthogonal system is used to define the local z axis.

The Global coordinate system is defined in the form of a natural coordinate ξ. The value of ξ is -1, 0 and 1 on the three faces of the element. Let 'P' be a point on the axis of the element and $r = X.i + Y.j + Z.k$ represents its position vector, then a unit tangent vector in x direction is defined as,

$$e_x = J^{-1}\left(\frac{\partial X}{\partial \xi} i + \frac{\partial Y}{\partial \xi} j + \frac{\partial Z}{\partial \xi}\, k\right)$$

The unit vectors along global X, Y and Z are represented by i, j and k in the above equation. The Jacobian factor is defined as,

$$J = \left[\left(\frac{\partial X}{\partial \xi}\right)^2 + \left(\frac{\partial Y}{\partial \xi}\right)^2 + \left(\frac{\partial Z}{\partial \xi}\right)^2\right]^{1/2}$$

2.2. Relationship between stress and strain

The displacements are defined in local as well as global coordinate system. The displacements in the local coordinate system are written as,

$$\bar{\delta} = \left[u, v, w, \theta_x, \theta_y, \theta_z, \theta_x', \gamma_d, \gamma_d'\right]^T$$

In the above equation, the translations in the local x, y and z axes are represented by u, v and w respectively, the twisting angle by θ_x, the twisting rate by θ_x', rotation around y and z axes by θ_y and θ_z respectively, the angle of distortion by γ_d and the distortion rate by γ_d'.

The above displacements are also defined in the global coordinate system as,

$$\delta = \left[U, V, W, \varphi_x, \varphi_y, \varphi_z, \theta_x', \gamma_d, \gamma_d'\right]$$

In the above equation, the translations in the global x, y and z axes are represented by U, V and W respectively and the rotations around the same axes by φ_x, φ_y and φ_z respectively. The twisting rate θ_x', the angle of distortion γ_d and the distortion rate γ_d' remains in local coordinate system as earlier. It is therefore evident that there are nine degrees of freedom per node of the thin-walled box beam element.

The stress vector in its general form is given by,

$$\sigma = \left[N_x, Q_y, Q_z, M_{st}, M_y, M_z, \frac{1}{\mu_t} B_1, M_d, B_{11}\right]^T$$

In the above equation, the axial force is represented by N_x, shear forces by Q_y and Q_z, pure torsional moment by M_{st}, primary bending moments by M_y and M_z, warping shear parameter by μ_t, torsional warping bi-moment by B_1, distortional moment by M_d and distortional warping bi-moment by B_{11}.

The strain vector in its general form is given by,

$$\varepsilon = \left[\varepsilon_x, \varepsilon_{yx}, \varepsilon_{zx}, \psi_{\theta x}, \psi_{yx}, \psi_{zx}, \psi_{wtx}, \psi_{dx}, \psi_{wdx}\right]^T$$

The different parameters in the above equation are defined as follows:

Axial strain, $\varepsilon_x = \frac{\partial u}{\partial x}$

Shear strain in y-direction, $\varepsilon_{yx} = \frac{\partial v}{\partial x} + \frac{\partial u}{\partial y} = \frac{\partial v}{\partial x} - \theta_z$

Shear strain in z-direction, $\varepsilon_{zx} = \frac{\partial w}{\partial x} + \frac{\partial u}{\partial z} = \frac{\partial w}{\partial x} + \theta_y$

Torsional strain, $\psi_{\theta x} = \frac{\partial \theta_x}{\partial x}$

Flexural strain about y-axis, $\psi_{yx} = \frac{\partial^2 u}{\partial x \partial z} = \frac{\partial \theta_y}{\partial x}$

Flexural strain about z-axis, $\psi_{zx} = \frac{\partial^2 u}{\partial x \partial y} = -\frac{\partial \theta_z}{\partial x}$

Torsional warping strain, $\psi_{wtx} = -\frac{\partial^2\theta_x}{\partial x^2} - \frac{1}{R}\frac{\partial\theta_z}{\partial x}$

$'R'$ in the above equation represents the radius of curvature and the torsional warping strain has been modified to consider the initial curvature effect.

Distortional strain, $\psi_{dx} = \gamma_d$

Distortional warping strain, $\psi_{wdx} = -\frac{\partial^2\gamma_d}{\partial x^2}$

The rigidity matrix in its generalized form is

$$D = \begin{bmatrix} EA & & & & & & & & \\ & GA_{sy} & & & & & 0 & & \\ & & GA_{sz} & & & & & & \\ & & & GJ_T & & & & & \\ & & & & EI_y & & & & \\ & & & & & EI_z & & & \\ & & 0 & & & & \frac{1}{\mu_t}E_1J_I & & \\ & & & & & & & E_1J_D & \\ & & & & & & & & E_1J_{II} \end{bmatrix}$$

In the above equation, Young's modulus of Elasticity is represented by E, shear modulus by G, the cross-sectional area by A, effective shear areas along y and z directions by A_{sy} and A_{sz} respectively, the torsional moment of inertia by J_T, the primary bending moments of inertia around y and z axes by I_y and I_z respectively, the torsional warping moment of inertia by J_I, warping shear parameter by μ_t, distortional second moment of area by J_d and the distortional warping moment of inertia by J_{II}. E_1 represents the conversion modulus of elasticity and is defined as,

$$E_1 = \frac{E}{(1-\nu^2)}$$

where, ν is the Poisson's ratio.

2.3. Shape functions

The axial and flexural effects require only C_0 continuity and the shape functions are given as,

$N_1 = \frac{1}{2}(\xi^2 + \xi_0)$ for i= 1 and 3

$N_1 = (1 - \xi_0)$ for i= 2

where, $\xi_0 = \xi\xi_1$

Since the governing equations for torsion and distortion are fourth order and the beam being three-noded, fifth order C_1 continuity is required for torsion and distortion. The shape functions are given as,

$$N_{11} = \left(\frac{\xi^2}{4}\right)(4 - 5\xi - 2\xi^2 + 3\xi^2)$$

$$N_{12} = \left(\frac{J_1}{4}\right)\xi^2(1 - \xi)(1 - \xi^2)$$

$$N_{21} = \left(\frac{\xi^2}{4}\right)(4 + 5\xi - 2\xi^2 + 3\xi^2)$$

$$N_{22} = \left(\frac{J_2}{4}\right)\xi^2(1 + \xi)(\xi^2 - 1)$$

$$N_{31} = (1 - \xi^2)^2$$

$$N_{32} = J_3\xi(1 - \xi^2)^2$$

where, $\xi_0 = \xi\xi_1$ and J_1, J_2 and J_3 are the Jacobian factors at the three nodes of the element.

The element stiffness matrix may be written as,

$$[K^e] = \int_{-1/2}^{1/2}[B]^T[D][B]\,dx = \int_{-1}^{1}J[B]^T[D][B]d\xi$$

The internal and external forces are represented in the form of nodal force vector given as,

$$[f^e] = \int_1[N]^T b\,dx + \int_1[N]^T q\,dx + \sum[N]^T P + \int_1[B]^T[D]\varepsilon_0 - \int_1[B]^T\sigma_0\,dx$$

where, b, q, P, ε_0 and σ_0 are the vectors representing body force, distributed force concentrated force, initial strain and initial stress respectively.

3. Numerical validation

A problem relating to the static analyses of steel box-girder has been discussed in order to validate the finite element formulation adopted in this study.

An eccentric point load applied on a curved steel box-girder

Originally taken from Zhange [17], this numerical example considers a simply supported box-girder of span 30.10 m with radius of curvature 76.2 m, the results of which are verified here through Matlab coding. The various sectional properties are presented in Table 1, while Figure 2 depicts a point load of 4450 N acting eccentrically over the right web, midway of the span. The percentage deviation of previous and present research parameters can be seen in Table 2. A total of 30 thin-walled box girder elements were used to obtain different response parameters. Figures 3(a)-(f) illustrates some important response parameters, such as vertical deflection, rotations about x and z axis, rate of rotation about x axis, distortional angle and rate of distortional angle. Also, different stress resultants like bending moment, shear force, torsional moment, torsional bi-moment, distortional moment and distortional bi-moment are shown in Figures 3(g)-(l).

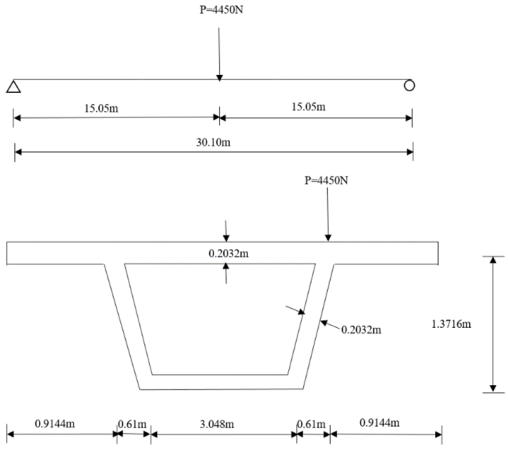

Fig. 2. Curved beam model with loading and dimensions

Table 1.
Different material properties [17]

Sectional Property	Value
E	2.45 e+11 N/m^2
ν	0.30
G	9.42 e+10N/m^2
I_z	9.41e-1 m^4
J_T	2.01 m^4
J_I	1.87e-1 m^6
J_{II}	4.45e-1 m^6
J_d	2.32e-3 m^2
μ_t	0.236
A	2.4305 m^2

Table 2.
Deviation between previous and present studies

Parameters	Zhang [17]	Authors	Deviation, %
Bending moment	-3.4*104 N-m	-3.5*104 N-m	2.94
Torsional bi-moment	1.1*103 N-m2	1.075*103 N-m2	2.27
Distortional bi-moment	6*103 N-m2	6.1*103 N-m2	1.67
Distortional moment	2.4*103 N-m	2.4*103 N-m	-

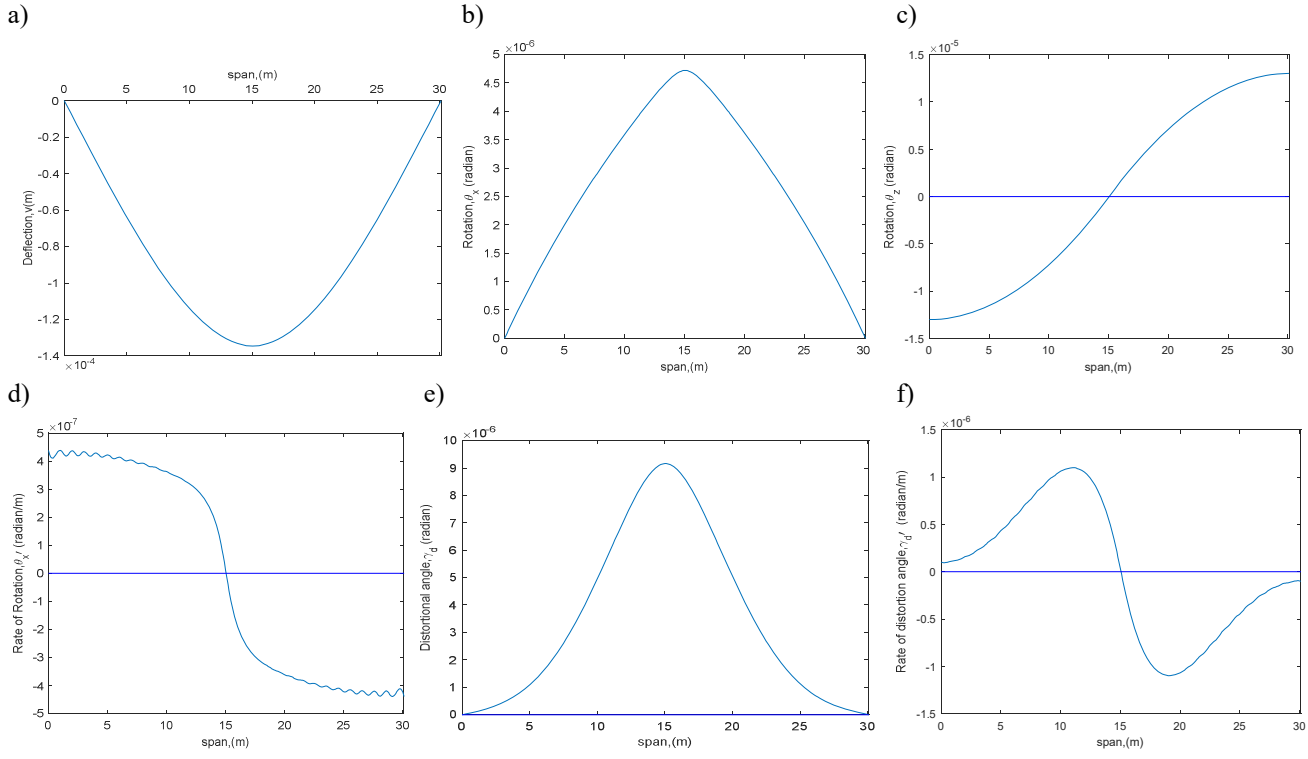

Fig. 3. a) Vertical deflection (v), b) rotation about x (θ_x), c) rotation about z (θ_z), d) rate of rotation about x (θ_x'), e) distortion angle (γ_d), f) rate of distortion angle (γ_d')

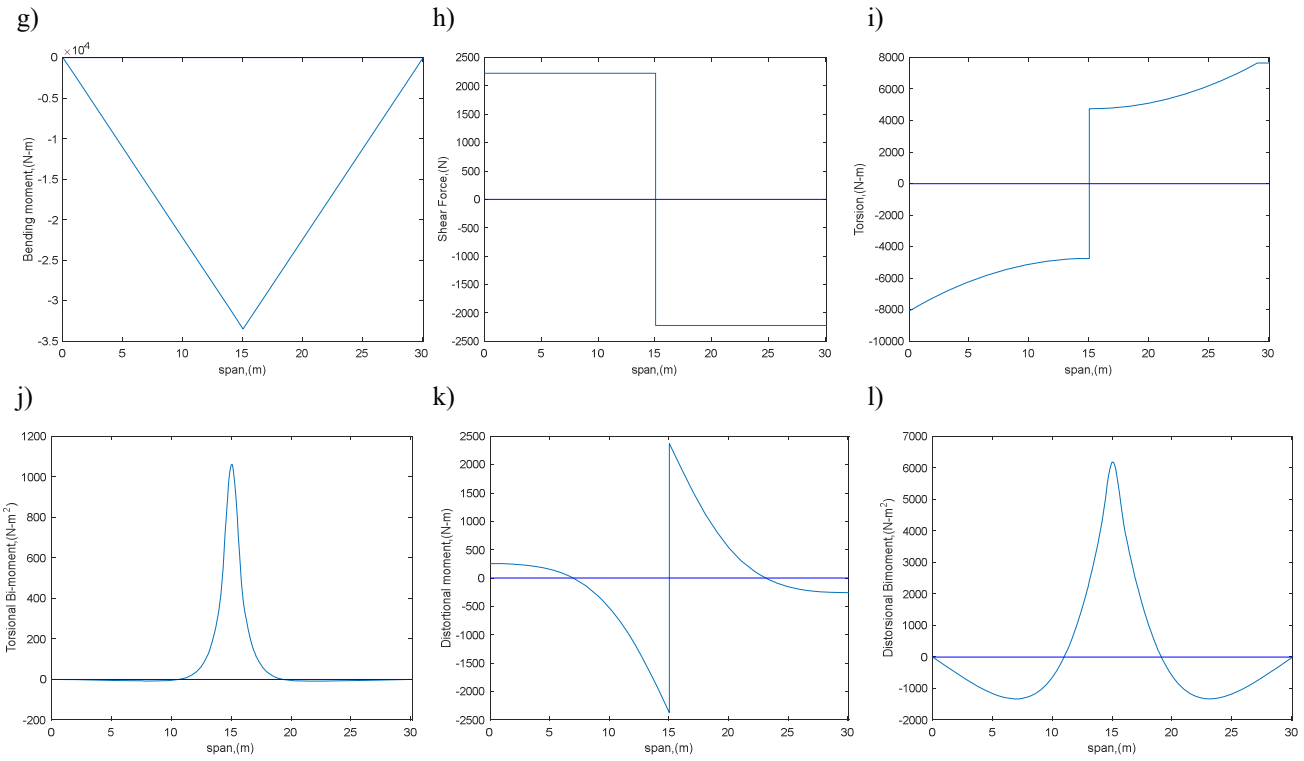

Fig. 3. (*cont.*) g) bending moment (M_z), h) shear force (Q_y), i) torsional moment (M_x), j) torsional bi-moment (B_1), k) distortional moment (M_d), l) distortional bi-moment (B_{11})

Table 3.
Different material properties [18]

Sectional Property	Value
E	2.068e+11 N/m^2
ν	0.29310
G	7.997e+10 N/m^2
I_z	1.1457e-2 m^4
J_T	2.3642e-2 m^4
J_I	9.7758e-4 m^6
J_{II}	2.0577e-3 m^6
J_d	6.00486e-6 m^2
μ_t	2.0309e-1
A	0.16048 m^2

4. Results and discussion

A Steel curved box-girder subjected to Indian standard railway loading

This numerical problem involves a simply supported steel curved box-girder bridge spanning 30.1 m with a curvature radius of 30.48 m and subjected to standard Indian railway loading for Broad Gauge. A total of seven internal Diaphragms are placed at 1/8th of span length. Figure 4 shows the cross-section and loading. The various sectional properties are presented in Table 3 and the different load combinations taken according to [19] are depicted in Figures 5-9.

The dead load of rail and ballast is taken as a uniformly distributed load of 24416.79 N/m and that of sleeper is taken as a point load of 2618.37 N at a distance of 0.6m.

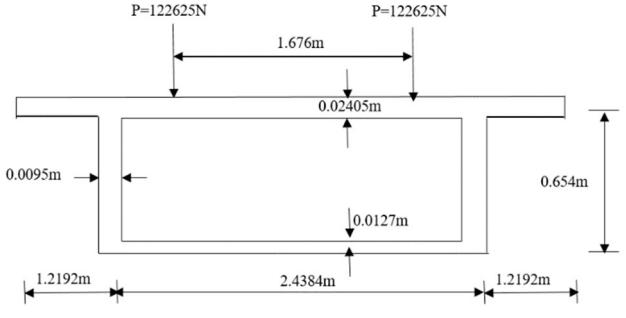

Fig. 4. Cross-section and loading

The centre of gravity of load and box-girder coincides in case of symmetrical loading, whereas for non-symmetrical loading the left load is at a distance of 0.419 m and right load at a distance of 1.257 m from centre of gravity of box-girder.

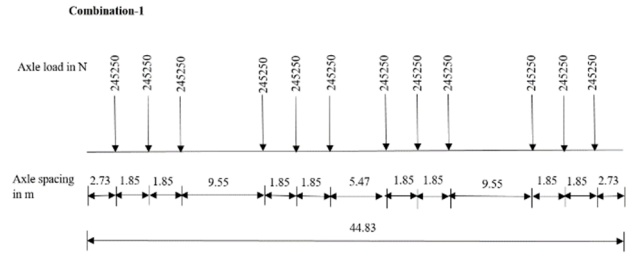

Fig. 5. Double headed diesel loco

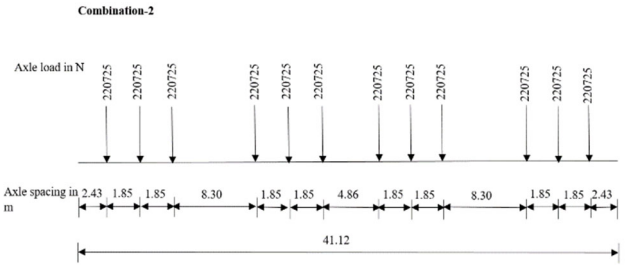

Fig. 6. Double headed electric loco

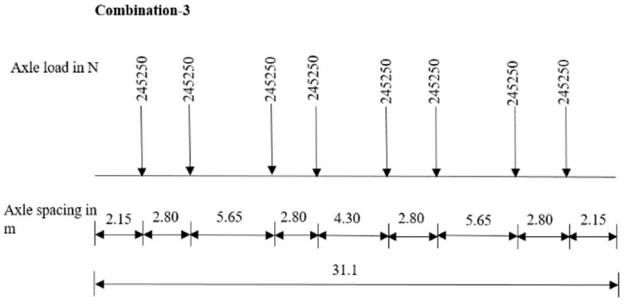

Fig. 7. Electric loco [(bo-bo) + (bo-bo)]

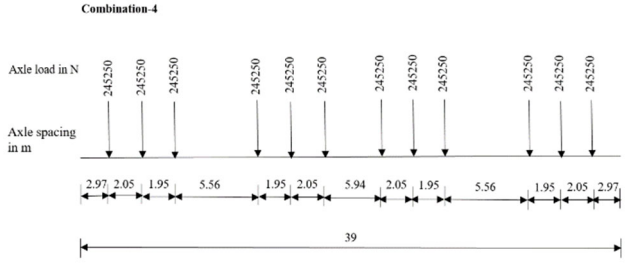

Fig. 8. With double headed 245250 loco

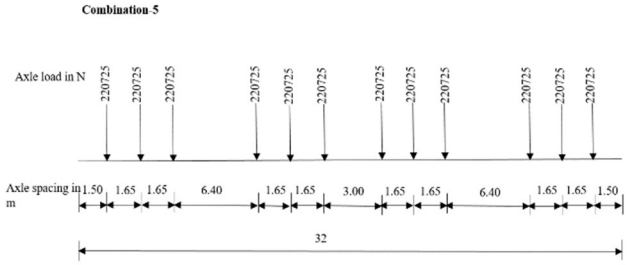

Fig. 9. With double headed 220725 loco

Figures 10(a)-(f) illustrates some important response parameters, such as vertical deflection, rotations about x and z axis, rate of rotation about x axis, distortional angle and rate of distortional angle. Also, different stress resultants like bending moment, shear force, torsional moment, torsional bi-moment, distortional moment and distortional bi-moment are shown in Figures 10(g)-(l).Variations in different stress resultants resulting from five different load combinations for symmetrical and non-symmetrical loading can be seen in Tables 4 and 5.

Table 4 and Table 6 clearly shows that Load combination 5 has the highest value of vertical deflection, shear Force and Bending Moment. The other stress resultants including Torsional moment, Distortional moment, Distortional bi-moment and Torsional bi-moment are not applicable due to symmetric nature of the load.

Table 5 and Table 7 reveals that Load combination 5 has the maximum value vertical deflection, rotation about x and z axis, rate of rotation about x axis, distortional angle, rate of distortional angle, shear force, bending moment, and torsion, while Load combination 1 has the highest value of distortion components such as distortion moment distortion moment and distortion bi-moment.

The variation of response parameters for fifth load combination non-symmetric load case with span ranging from 15 m to 30.1 m is presented in Table 8 and Table 9. An investigation of the values shows that as the span length increases, various stress resultants such as shear force, bending moment, torsion and torsional bi-moment increase. The variation in distortion components like distortional angle, rate of distortional angle, distortion moment and distortion bi-moment is found to be non-linear.

The results also show that as the span length increases, the value of vertical deflection, rotation about x and z axis and rate of rotation about x axis increase.Table 10 and Table 11 demonstrates the variation of response parameters arising from fifth load combination of non-symmetric load case with curvature radius ranging from 30.48 m to ∞. It is interesting to note that torsion related stresses have increased significantly as the radius of curvature decreases.

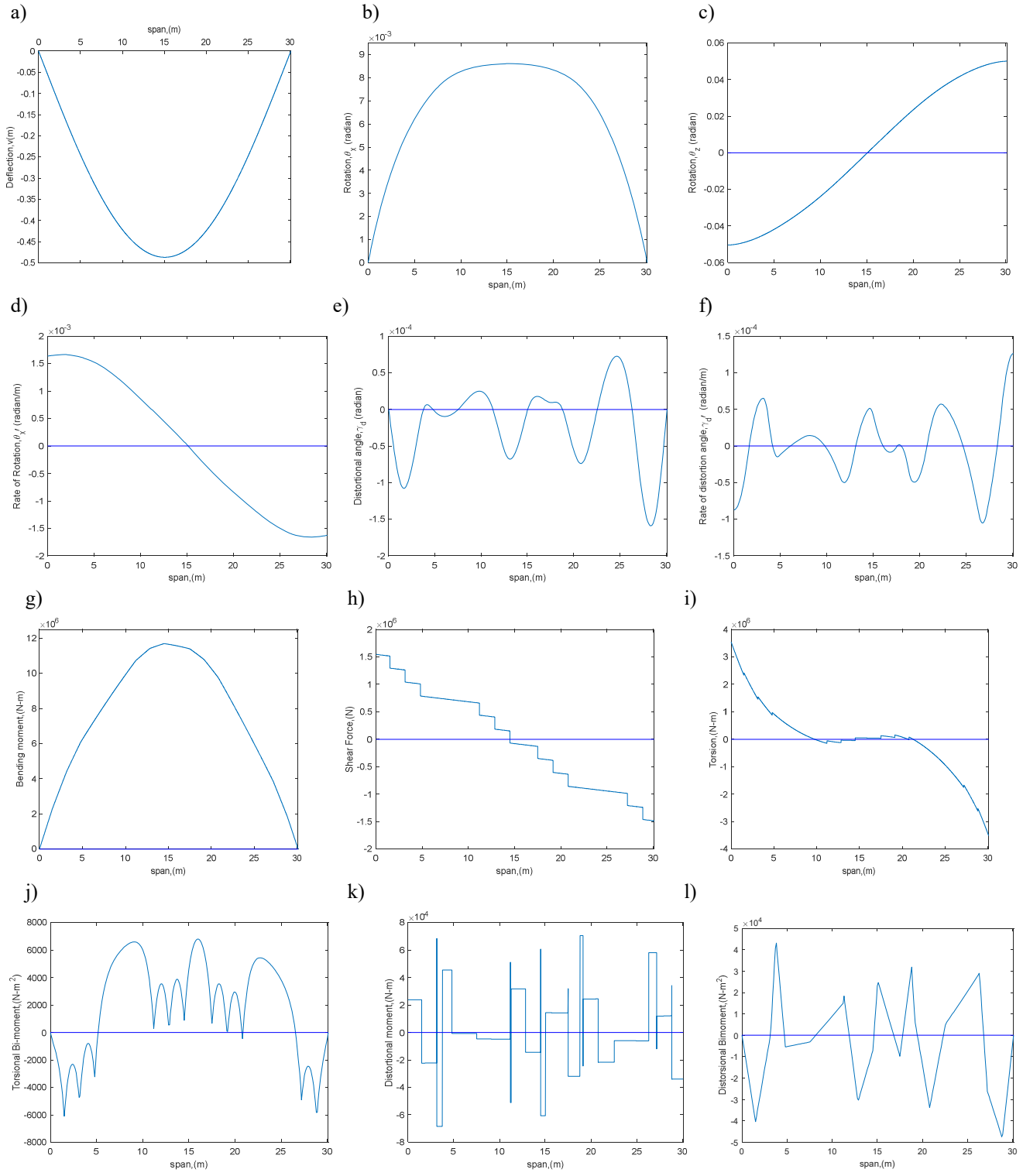

Fig. 10. a) Vertical deflection (v), b) rotation about x (θ_x), c) rotation about z (θ_z), d) rate of rotation about x (θ_x'), e) distortion angle (γ_d), f) rate of distortion angle (γ_d'), g) bending moment (M_z), h) shear force (Q_y), i) torsional moment (M_x), j) torsional bi-moment (B_1), k) distortional moment (M_d), l) distortional bi-moment (B_{11})

Table 4.
Different response parameters for symmetric loading

Combination / Response parameter	Combination 1	Combination 2	Combination 3	Combination 4	Combination 5
Q_y (N)	-1.51e+6	-1.29e+6	-1.31e+6	-1.37e+6	-1.54e+6
M_z (N-m)	9.84e+6	9.98e+6	9.43e+6	11.19e+6	11.69e+6
M_x (N-m)	**	**	**	**	**
B_1 (N-m^2)	**	**	**	**	**
M_d (N-m)	**	**	**	**	**
B_{11} (N-m^2)	**	**	**	**	**
** Not applicable due to symmetric nature of the load					

Table 5.
Different response parameters for non-symmetric loading

Combination / Response parameter	Combination 1	Combination 2	Combination 3	Combination 4	Combination 5
Q_y (N)	-1.50e+6	-1.29e+6	-1.31e+6	-1.37e+6	-1.54e+6
M_z (N-m)	9.84e+6	9.98e+6	9.43e+6	11.19e+6	11.69e+6
M_x (N-m)	-3.10e+6	-3.18e+6	-2.92e+6	-3.48e+6	-3.50e+6
B_1 (N-m^2)	6.86e+3	6.62e+3	6.37e+3	7.35e+3	6.80e+3
M_d (N-m)	71.03e+3	62.43e+3	51.57e+3	68.69e+3	70.60e+3
B_{11} (N-m^2)	47.08e+3	36.26e+3	35.40e+3	38.2e+3	43.12e+3

Table 6.
Different response parameters for symmetric loading

Combination / Response parameter	Combination 1	Combination 2	Combination 3	Combination 4	Combination 5
v (m)	-417.82e-3	-421.28e-3	-405.08e-3	-475.64e-3	-491.23e-3
θ_x (radian)	**	**	**	**	**
θ_z (radian)	44.40e-3	44.39e-3	41.81e-3	49.18e-3	50.20e-3
θ_x' (radian/m)	**	**	**	**	**
γ_d (radian)	**	**	**	**	**
γ_d' (radian/m)	**	**	**	**	**
** Not applicable due to symmetric nature of the load					

Table 7.
Different response parameters for non-symmetric loading

Combination / Response parameter	Combination 1	Combination 2	Combination 3	Combination 4	Combination 5
v (m)	-413.88e-3	-417.37e-3	-401.43e-3	-471.13e-3	-486.64e-3
θ_x (radian)	7.06e-3	7.21e-3	7.09e-3	8.19e-3	8.60e-3
θ_z (radian)	44.29e-3	44.29e-3	41.70e-3	49.05e-3	50.06e-3
θ_x' (radian/m)	-1.46e-3	-1.48e-3	-1.39e-3	-1.62e-3	-1.66e-3
γ_d (radian)	-120.03e-6	-76.41e-6	-99.39e-6	-71.36e-6	-159.01e-6
γ_d' (radian/m)	102.5e-6	57.32e-6	89.82e-6	60.17e-6	126.4e-6
** Not applicable due to symmetric nature of the load					

Table 8.
Stress resultants for varying span length

Length of span(L) in m				
Response parameter	15	20	25	30
Q_y (N)	857.90e+3	1.03e+6	1.31e+6	1.54e+6
M_z (N-m)	2.36e+6	4.97e+6	8.34e+6	11.69e+6
M_x (N-m)	-127.37e+3	-765.91e+3	-2.0e+6	-3.5e+6
B_1 (N-m^2)	1.55e+3	3.22e+3	5.03e+3	6.80e+3
M_d (N-m)	58.44e+3	80.03e+3	67.10e+3	70.60e+3
B_{11} (N-m^2)	41.08e+3	33.53e+3	35.21e+3	43.12e+3

Table 9.
Stress resultants for varying span length

Length of span(L) in m				
Response parameter	15	20	25	30
v (m)	-25.10e-3	-88.93e-3	-234.14e-3	-486.64e-3
θ_x (radian)	102.27e-6	1.02e-3	3.57e-3	8.61e-3
θ_z (radian)	5.45e-3	14.52e-3	29.85e-3	50.06e-3
θ_x' (radian/m)	-0.11e-3	-0.41e-3	-0.97e-3	-1.6e-3
γ_d (radian)	-65.33e-6	-62.69e-6	-73.04e-6	-159.01e-6
γ_d' (radian/m)	70.65e-6	45.66e-6	50.73e-6	126.4e-6

Table 10.
Stress Resultants for varying radius of curvature

Radius of curvature(R) in m					
Response parameter	30.48	60.96	121.92	243.84	∞
Q_y (N)	1.54e+6	1.54e+6	1.54e+6	1.54e+6	1.54e+6
M_z (N-m)	11.69e+6	11.69e+6	11.69e+6	11.69e+6	11.69e+6
M_x (N-m)	-3.5e+6	-1.38e+6	-433.27e+3	-231.73e+3	-521.17e+3
B_1 (N-m^2)	6.80e+3	3.14e+3	1.43e+3	0.59e+3	24.21e-9
M_d (N-m)	70.60e+3	70.13e+3	70.03e+3	70.01e+3	70.01e+3
B_{11} (N-m^2)	43.12e+3	40.14e+3	39.49e+3	39.34e+3	39.29e+3

Table 11.
Stress resultants for varying radius of curvature

Radius of curvature(R) in m					
Response parameter	30.48	60.96	121.92	243.84	∞
v (m)	-486.64e-3	-461.41e-3	-456.35e-3	-455.39e-3	-455.32e-3
θ_x (radian)	8.61e-3	2.95e-3	685.13e-6	633.57e-6	620.42e-6
θ_z (radian)	50.06e-3	48.32e-3	47.93e-3	47.84e-3	47.83e-3
θ_x' (radian/m)	-1.6e-3	-0.73e-3	-0.27e-3	-0.05e-3	-0.26e-3
γ_d (radian)	-159.01e-6	-127.11e-6	-120.83e-6	-119.35e-6	-118.86e-6
γ_d' (radian/m)	126.4e-6	109.6e-6	106.10e-6	105.47e-6	105.01e-6

Table 12.
Chemical composition of steel

Type of steel	Standard structural steel
Designation	Fe 410 B
IS code	2062
Carbon (%)	0.22
Manganese (%)	1.5
Sulphur (%)	0.045
Phosphorus(%)	0.045
Silicon(%)	0.4

It is therefore important to increase the torsional stiffness of the bridge as the curvature radius decreases. Flexural components such as bending moment and shear force are seen to remain unchanged, whereas the distortion components change marginally. The results also show that as the radius increases, the value of vertical deflection, rotation about x and z axis and rate of rotation about x axis decrease. Table 12 shows the Fe 410 B standard structural steel, that has been used in the current study, as specified in [20]. The table also includes a breakdown of the various chemical components, as well as their maximum percentages. The ultimate tensile strength and Yield strength of the steel are 4.1 e+8 N/m^2 and 2.5 e+8 N/m^2 respectively.

5. Conclusions

The work implemented in this article takes into consideration the thin-walled beam element originally introduced by Zhang and Lyons [15] for the static analysis of thin-walled box-girder bridges subjected to Indian railway loading. Using the three noded, one-dimensional beam element, a variety of structural actions such as torsional warping, distortion, bending and torsion of thin-walled box-girder bridge have been examined. The coding has been done in MATLAB, providing numerical results for different load cases.The key aspects of the work presented can be concluded in the following points:

1. The numerical results are in excellent agreement with the work of previous investigators, with a maximum divergence of 2.94 percent and hence validating the finite element methodology implemented in the present analysis.
2. The algorithm employed is appropriate for assessing both straight and curved steel box-girder bridges. Importantly, the Matlab code can include a variety of boundary conditions with or without diaphragms.
3. The increase in radius induces a decrease in all degrees of freedom with a maximum reduction of 92.79% in rotation along *x* axis and causes a decrease in torsion-related stress resultants only with a maximum reduction of 100% in torsional bi-moment.
4. The increase in span length results in an increase in nearly all degrees of freedom with a maximum increase of 98.81% in rotation around *x* axis and an increase in almost all the resulting stresses with a maximum increase of 76.36% in torsional moment.
5. The results clearly show that all degrees of freedom and the resulting stress such as shear force, bending moment, and torsion are found to be maximum in load combination 5.

References

[1] V.Z. Vlasov, Beams TW Chapter V, National Science Foundation, Washington, DC, 1961.

[2] B.I. Maisel, Analysis of concrete box beams using small computer capacity, Canadian Journal of Civil Engineering 28/1 (1985) 265-278. DOI: https://doi.org/10.1139/l85-028

[3] K. Hasebe, S. Usuki, Y. Horie, Shear lag analysis and effective width of curved girder bridges, Journal of Engineering Mechanics 111/1 (1985) 87-92. DOI: https://doi.org/10.1061/(ASCE)0733-9399(1985)111:1(87)

[4] B.A. Burgan, P.J. Dowling, The treatment of shear lag in design, Thin-Walled Structures 9/1-4 (1990) 121-134. DOI: https://doi.org/10.1016/0263-8231(90)90041-V

[5] J. Jönsson, Distortional warping functions and shear distributions in thin-walled beams, Thin-Walled Structures 33/4 (1999) 245-268. DOI: https://doi.org/10.1016/S0263-8231(98)00048-2

[6] G.C. Ezeokpube, S.B. Singh, N.N. Osadebe, Numerical and Experimental Modeling of the Static Response of Simply Supported Thin-Walled Box Girder Bridges, Nigerian Journal of Technology 34/4 (2015) 685-698. DOI: https://doi.org/10.4314/njt.v34i4.4

[7] K. Kashefi, A.H. Sheikh, M.C. Griffith, M.M. Ali, K. Tateishi, Static and vibration characteristics of thin-walled box beams: an experimental investigation, Advances in Structural Engineering 20/10 (2017) 1540-1559. DOI: https://doi.org/10.1177/1369433216687565

[8] A. Fam, C. Turkstra, A finite element scheme for box bridge analysis, Computers and Structures 5/2-3 (1975) 179-186. DOI: https://doi.org/10.1016/0045-7949(75)90008-5

[9] L.F. Boswell, S.H. Zhang, The effect of distortion in thin-walled box-spine beams, International Journal of

Solids and Structures 20/9-10 (1984) 845-862. DOI: https://doi.org/10.1016/0020-7683(84)90054-4

[10] Y.Y. Kim, Y. Kim, A one-dimensional theory of thin-walled curved rectangular box beams under torsion and out-of-plane bending, International Journal for Numerical Methods in Engineering 53/7 (2002) 1675-1693. DOI: https://doi.org/10.1002/nme.357

[11] Z. Begum, Analysis and behaviour investigations of box girder bridges, PhD Thesis, University of Maryland, College Park, USA, 2010.

[12] Z. Zhu, L. Zhang, D. Zheng, G. Cao, Free vibration of horizontally curved thin-walled beams with rectangular hollow sections considering two compatible displacement fields, Mechanics Based Design of Structures and Machines 44/4 (2016) 354-371. DOI: https://doi.org/10.1080/15397734.2015.1075410

[13] T. Gupta, M. Kumar, Flexural response of skew-curved concrete box-girder bridges, Engineering Structures 163 (2018) 358-372. DOI: https://doi.org/10.1016/j.engstruct.2018.02.063

[14] B.A. Hamza, A.R. Radhi, Q. Al-Madhlom, Effect of (B/D) ratio on ultimate load capacity for horizontally curved box steel beam under out of plane concentrated load, Engineering Science and Technology, an International Journal 22/2 (2019) 533-537. DOI: https://doi.org/10.1016/j.jestch.2018.09.007

[15] S.H. Zhang, L.P.R. Lyons, A thin-walled box beam finite element for curved bridge analysis, Computers and Structures 18/6 (1984) 1035-1046. DOI: https://doi.org/10.1016/0045-7949(84)90148-2

[16] L.F. Boswell, S.H. Zhang, A box beam finite element for the elastic analysis of thin-walled structures, Thin-Walled Structures 1/4 (1983) 353-383. DOI: https://doi.org/10.1016/0263-8231(83)90014-9

[17] S.H. Zhang, The finite element analysis of thin-walled box spine-beam bridges, PhD Thesis, City University London, London, UK, 1982.

[18] C.P. Heins Jr, J.C. Oleinik, Curved box beam bridge analysis, Computers and Structures 6/2 (1976) 65-73. DOI: https://doi.org/10.1016/0045-7949(76)90054-7

[19] Government of India, Ministry of Railways (Railway Board) Bridge Rules, Rules Specifying the loads for design of Super-Structure and Sub-Structure of Bridges and for assessment of the strength of existing Bridges, Lucknow, 2014.

[20] Indian Standard, Hot Rolled Medium And High Tensile Structural Steel — Specification (Seventh Revision), Bureau of Indian standards, Manak Bhavan, 9 Bahadur Shah Zafar Marg, New Delhi, 2011.